Hindawi
Advances in Civil Engineering
Volume 2018, Article ID 7826156, 14 pages
https://doi.org/10.1155/2018/7826156

Research Article

Effects of Single and Hybrid Steel Fiber Lengths and Fiber Contents on the Mechanical Properties of High-Strength Fiber-Reinforced Concrete

Kyoung-Chul Kim,[1] In-Hwan Yang,[1] and Changbin Joh[2]

[1]*Department of Civil Engineering, Kunsan National University, Kunsan, Jeonbuk 54150, Republic of Korea*
[2]*Structural Engineering Research Institute, Korea Institute of Civil Engineering and Building Technology, Goyang, Gyeonggi 10223, Republic of Korea*

Correspondence should be addressed to In-Hwan Yang; ihyang@kunsan.ac.kr

Received 20 October 2017; Revised 28 January 2018; Accepted 13 February 2018; Published 22 March 2018

Academic Editor: Peng Zhang

This paper describes an experimental study on the mechanical properties of high-strength fiber-reinforced concrete (HSFRC). The experimental parameters included the content and length of the steel fiber as well as the use of either a single-type fiber or hybrid steel fibers. The steel fiber contents were 1.0, 1.5, and 2.0% based on the volume of HSFRC, and the steel fiber lengths were 13, 16.5, and 19.5 mm. In addition, hybrid steel fibers incorporating steel fibers of different lengths were used. Compression tests and crack mouth opening displacement tests were performed for each HSFRC mixture with different experimental parameters. The mechanical properties of the HSFRC, such as compressive strength, elastic modulus, and tensile strength, increased with the steel fiber content. The mechanical property results of the HSFRC mixture using a single fiber length of 13 mm were greater than the results of the other mixtures. The compressive strength, elastic modulus, and tensile strength of the HSFRC mixture with hybrid steel fibers were similar to those of the mixtures with a single length of steel fiber. Additionally, based on the test results of the material properties, equations for predicting the elastic modulus and tensile strength of the HSFRC were suggested; the predictions using the proposed formula closely agreed with the experimental results.

1. Introduction

High-strength fiber-reinforced concrete (HSFRC) has an improved particle size distribution due to the constituent materials, and the microstructural porosity of HSFRC is minimized by using fillers with fine aggregates. In addition, steel fibers are contained within the HSFRC. Therefore, the HSFRC characteristics, including compressive behavior, tensile behavior, and durability, are superior to those of conventional concrete [1, 2].

The results of previous studies have shown that the compressive strength of HSFRC is between 130 and 200 MPa. The amount and type of steel fiber used in the HSFRC affect its mechanical properties, with an elastic modulus between 45 and 55 GPa and a tensile strength between 10 and 20 MPa [3, 4]. Hassan et al. [5] carried out experiments to investigate the material properties of HSFRC by incorporating steel fiber contents of 0, 1.0, and 2.0%; the compressive strength, elastic modulus, and tensile strength increased as the steel fiber content and fiber-reinforcing index increased. Thus, HSFRC has a high compressive strength and elastic modulus, and it can compensate for the disadvantages of normal-strength concrete by increasing the tensile strength and improving the flexural toughness.

Most of the studies on HSFRC have been carried out with a single type of fiber. However, in recent years, the mechanical characteristics of steel fiber-reinforced concrete with hybrid steel fibers, which incorporate two different types of fiber or different lengths of steel fiber, were investigated [6–8]. Chan and Chu [9] studied the material properties of hybrid fiber-reinforced concrete using carbon fiber, polypropylene (PP) fiber, and steel fiber. Three types of hybrid fibers were tested: 0.2% carbon fiber and 0.3% steel fiber; 0.2% carbon fiber and 0.3% PP fiber; and 0.2% steel

Table 1: Mix proportions of the HSFRC.

Mixture	W/B	W	OPC	Zr	SF	BFS	FA	F	Steel fiber	
									Fiber content by volume (V_f) (%)	Diameter (D_f) (mm)
F10-S-L130	0.16	157	770	—	193	—	848	231	1.0 = 1.0 (13.0 mm)	0.2
F10-S-L195	0.22	209	770	58	—	135	847	231	1.0 = 1.0 (19.5 mm)	0.2
F10-H	0.16	157	770	—	193	—	848	231	1.0 = 0.5 (16.5 mm) + 0.5 (19.5 mm)	0.2
F15-S-L130	0.16	157	770	—	193	—	848	231	1.5 = 1.5 (13 mm)	0.2
F15-H(BFS)	0.18	180	788	99	—	99	867	236	1.5 = 0.5 (16.5 mm) + 1.0 (19.5 mm)	0.2
F15-H	0.18	178	783	196	—	—	862	235	1.5 = 0.5 (16.5 mm) + 1.0 (19.5 mm)	0.2
F20-S-L130	0.16	157	770	—	193	—	848	232	2.0 = 2.0 (13 mm)	0.2
F20-H	0.16	157	770	—	193	—	848	232	2.0 = 1.0 (16.5 mm) + 1.0 (19.5 mm)	0.2

Note. OPC: ordinary Portland cement; Zr: zirconium; SF: silica fume; BFS: blast-furnace slag; FA: fine aggregate; F: filler; and W: water.

fiber and 0.3% PP fiber. Although low fiber contents were used in these hybrid fibers, the use of hybrid fibers improved the strength and toughness of the concrete. In the Chan and Chu [9] study, the flexural strength and toughness of the specimen with the hybrid fiber containing carbon and steel fibers were greater than those of the other two hybrid fibers. Banthia and Tasdemir [10] studied the characteristics of concrete reinforced by steel fiber with a crimp shape, diameters of 0.40, 0.45, and 0.80 mm and a length of 30 mm. They evaluated the toughness of steel fiber-reinforced concrete with a single steel fiber and with two different types of hybrid steel fibers. The flexural toughness of the steel fiber-reinforced concrete fabricated with a hybrid steel fiber was less than that of steel fiber-reinforced concrete fabricated with a single small-diameter steel fiber. As the diameter of the steel fiber increased, the dispersion of the fiber in the concrete decreased, and the flexural toughness of the macrocrack decreased.

In addition, Akcay and Tasdemir [11] analysed the characteristics of steel fiber-reinforced concrete using different lengths of steel fiber. They conducted experimental studies using 0.75 and 1.5% steel fiber contents by volume. The use of a long fiber resulted in an increase in the flexural toughness of the steel fiber-reinforced concrete but did not affect its flexural strength because the degree of dispersion of the fibers decreased due to the geometric shape of the long fibers, which affected the workability. The results of the previous studies on concrete with hybrid steel fibers did not explicitly determine whether the use of hybrid steel fiber in fiber-reinforced concrete effectively improves the mechanical properties of HSFRC. Therefore, further studies on the effect of steel fiber characteristics, such as the type and length, on the mechanical properties of HSFRC concrete are needed.

Here, an experimental study on the mechanical properties of HSFRC was carried out using steel fibers with lengths of 13, 16.5, and 19.5 mm. Additionally, the effects of different fiber types including single and hybrid steel fibers as well as the contents on the HSFRC were evaluated.

2. Mix Proportions

Table 1 shows the mix proportions of HSFRC used in this study. The cement used in the mixture was ordinary Portland cement (OPC). In addition to OPC, zirconium, silica fume, and blast-furnace slag were used as binders. Unlike conventional concrete, HSFRC does not contain coarse aggregate but includes filler. The fine aggregate has a diameter of 0.5 mm or less, and the average diameter of the filler is 4 μm. The filler contains more than 96% SiO_2, and the density of the filler is 2.60 g/cm^3. The water-binder ratio (w/b) is between 0.16 and 0.22. A polycarboxylic acid-based high-performance water-reducing agent with a density of 1.01 g/cm^3 was used to ensure the workability due to a low water-binder ratio.

HSFRC also includes steel fiber. The contents, type, and lengths of the fiber are different in each mixture. The steel fibers were 1.0, 1.5, and 2.0% based on the volume of the mixture; in Table 1, F10, F15, and F20 represent the percentages of steel fiber content, respectively. The HSFRC in this study is divided into two categories. One category of HSFRC uses a single type of fiber, and the other category of HSFRC uses a hybrid fiber. Hybrid fiber consists of steel fibers of two lengths. The density of the steel fiber is 7,500 kg/cm^3, and the tensile strength is 2,500 MPa. Straight steel fibers with a diameter of 0.2 mm and lengths of 13, 16.5, and 19.5 mm were used in this study, as shown in Figure 1. In Table 1, S and H denote a single steel fiber and a hybrid steel fiber, respectively. Additionally, L130 and L195 denote steel fiber lengths of 13 and 19.5 mm, respectively.

3. Compressive Strength and Elastic Modulus

A cylindrical specimen with a diameter of 100 mm and a height of 200 mm was fabricated from each mixture. The specimens were wet cured for the first day after casting, and then, steam curing was carried out at 90 ± 5°C for 72 hours. After the samples were steam cured, wet curing was carried out for 28 days after specimen fabrication.

Three linear displacement transducers (LVDTs) were installed around the cylindrical specimen, with a distance of 100 mm between the attachment points. The displacement was measured during loading, as shown in Figure 2. The compressive stress-strain curves and elastic modulus of the HSFRC were calculated by using the load-displacement relation measured from the compressive strength test. The stress-strain relationship of the HSFRC was nearly linear until the maximum strain stage was reached. Graybeal [12] determined the elastic modulus by using the compressive stress, corresponding to 10% and 30% of the ultimate

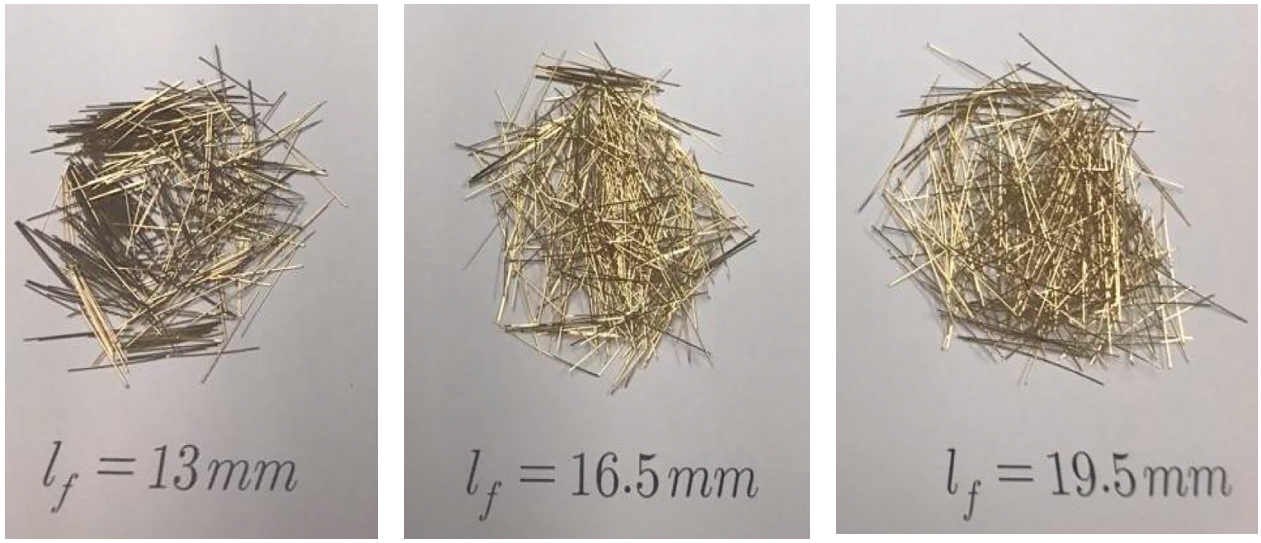

(a) (b) (c)

Figure 1: Steel fiber used in this study. (a) $l_f = 13$ mm. (b) $l_f = 16.5$ mm. (c) $l_f = 19.5$ mm.

Figure 2: Compressive strength test.

compressive strength. In this study, the elastic modulus was calculated by applying Graybeal's method.

The mean compressive strength and elastic modulus of the F10-S-L130, F10-S-L195, and F10-H mixtures are shown in Table 2. The mean compressive strength of the 13 specimens of the F10-S-L130 mixture was 173.0 MPa and that of the 23 specimens of the F10-S-L195 mixture was 133.7 MPa; the mean elastic modulus values of these mixtures were 44,145, and 40,147 MPa, respectively. The F10-S-L130 and F10-S-L195 mixtures contained the same percentages of steel fibers (1.0%) but different water-binder ratios and fiber lengths. The lengths of the steel fibers of the two mixtures were 13 mm and 19.5 mm, respectively, and the water-binder ratios of the two mixtures were 0.16 and 0.22, respectively. The compressive strength and elastic modulus of the F10-S-L195 mixture were smaller than those of the F10-S-L130 mixture. Because the high water-binder ratio of the concrete can reduce the compressive strength and elastic modulus, the different water-binder ratios may be the reason for the reductions in the compressive strength and elastic modulus. In addition, the dispersion of steel fibers might affect the compressive strength and elastic modulus of the HSFRC. The decreases in the compressive strength and elastic modulus could result from the decrease in the dispersion of the steel fibers in the HSFRC due to the use of longer steel fibers. The results of Yoo et al. [13] indicated that the use of longer fibers resulted in a decrease in their dispersion, and the experimental results of this study are similar. In addition, blast-furnace slag binders are relatively disadvantageous for short-term strength development but advantageous for long-term strength development [14]. The containment of blast-furnace slag in the F10-S-L195 mixture adversely affected the compressive strength and elastic modulus at 28 days.

In contrast, the mean compressive strength of the F10-S-L130 and F10-H mixtures was 173.0 and 174.0 MPa, respectively, and the mean elastic modulus of each mixture was 44,145 and 43,550 MPa, respectively. The compressive strength and the elastic modulus of the two mixtures did not show any significant differences. The two mixtures had the same water-binder ratio of 0.16, meaning that they had the same concrete mixing proportions but different fiber lengths with the same fiber content of 1.0%. This indicates that the use of hybrid steel fibers (16.5 and 19.5 mm) and short fibers (13 mm) in the HSFRC had approximately the same effect on the compressive strength and elastic modulus of the HSFRC.

The mean compressive strength and elastic modulus of the F15-S-L130, F15-H(BFS), and F15-H mixtures are shown in Table 3. Compressive strength tests were conducted on 16 specimens of the F15-S-L130 mixture, 9 specimens of the F15-H(BFS) mixture, and 18 specimens of the F15-H mixture. The mean compressive strength of each mixture was 188.5, 148.8, and 181.2 MPa, respectively. The elastic modulus values for the F15-SL130 and F15-H(BFS) mixtures were 45,996 and 43,217 MPa, respectively. The elastic modulus of the F15-H mixture was not measured due to an equipment problem related to the LVDTs.

Table 2: Test results of the compressive strength and elastic modulus (V_f = 1.0%).

Mixture	Batch	Number of specimens	Fiber content V_f (%)	Compressive strength ($f_{c,mean}$) (MPa)	Elastic modulus ($E_{c,mean}$) (MPa)
F10-S-L130	1	4	1.0	174.6	43,551
	2	3	1.0	181.3	45,561
	3	2	1.0	168.9	43,396
	4	4	1.0	167.2	44,051
	Mean			173.0	44,145
F10-S-L195	1	5	1.0	121.6	41,469
	2	5	1.0	138.5	39,936
	3	4	1.0	137.1	39,192
	4	4	1.0	134.6	39,081
	5	5	1.0	137.4	40,652
	Mean			133.7	40,147
F10-H	1	5	1.0	174.0	43,550
	Mean			174.0	43,550

Table 3: Test results of the compressive strength and elastic modulus (V_f = 1.5%).

Mixture	Batch	Number of specimens	Fiber content V_f (%)	Compressive strength ($f_{c,mean}$) (MPa)	Elastic modulus ($E_{c,mean}$) (MPa)
F15-S-L130	1	4	1.5	188.2	45,930
	2	4	1.5	183.6	45,849
	3	4	1.5	193.0	46,924
	4	4	1.5	189.2	45,281
	Mean			188.5	45,996
F15-H(BFS)	1	4	1.5	169.2	48,334
	2	5	1.5	132.5	39,123
	Mean			148.8	43,217
F15-H	1	3	1.5	182.9	—
	2	3	1.5	179.9	—
	3	3	1.5	181.9	—
	4	3	1.5	177.8	—
	5	3	1.5	178.6	—
	6	3	1.5	186.1	—
	Mean			181.2	—

The F15-S-L130 mixture contained 1.5% of steel fibers with a length of only 13 mm, and the F15-H mixture contained hybrid steel fibers with lengths of 16.5 and 19.5 mm. The compressive strength of the F15-S-L130 mixture with short fibers was not significantly different from that of the F15-H mixture with hybrid steel fibers, indicating that the compressive strength of the HSFRC including hybrid steel fibers with lengths of 16.5 and 19.5 mm and the HSFRC containing a single type of steel fiber with a length of only 13 mm was approximately equal. These characteristics are also similar to the compressive strength characteristics of the F10 series mixtures containing 1.0% of steel fibers, as previously explained.

The F15-H(BFS) mixture contained 1.5% hybrid steel fibers with lengths of 16.5 and 19.5 mm and the blast-furnace slag. The compressive strength of the F15-H(BFS) mixture was less than that of the F15-H mixture, indicating that the incorporation of blast-furnace slag adversely affected the strength of the HSFRC.

The mean compressive strength and elastic modulus of the F20-S-L130 and F20-H mixtures are shown in Table 4. The mean values of the compressive strength of the F20-S-L130 (39 specimens) and F20-H (21 specimens) mixtures was 180.7 and 181.9 MPa, respectively, and the mean values of the elastic modulus of each mixture were 47,016 and 44,267 MPa, respectively. The two mixtures had the same water-binder ratio and the same steel fiber content based on the volume of concrete but different steel fiber lengths. The F20-S-L130 mixture contained 2% steel fiber volume with a length of only 13 mm, and the F20-H mixture contained 1.0% steel fiber volume with a length of 16.5 mm as well as 1.0% steel fiber volume with a length of 19.5 mm. The compressive strength of the F20-S-L130 mixture with a single type of short fiber was almost the same as that of the F20-H mixture with hybrid steel fibers, indicating that the use of hybrid steel fibers in the HSFRC did not adversely affect the HSFRC compressive strength. These characteristics are also similar to the compressive strength characteristics of the F10 series mixtures containing 1.0% steel fibers, as previously explained. In contrast, the mean of the elastic modulus of the HSFRC with the hybrid steel fibers was reduced by 5.8% compared with the mixture with a single type of steel fiber.

Table 4: Test results of the compressive strength and elastic modulus (V_f = 2.0%).

Mixture	Batch	Number of specimens	Fiber content V_f (%)	Compressive strength ($f_{c,mean}$) (MPa)	Elastic modulus ($E_{c,mean}$) (MPa)
F20-S-L130	1	3	2.0	158.2	46,880
	2	3	2.0	188.4	45,894
	3	6	2.0	177.9	47,650
	4	6	2.0	175.5	49,212
	5	5	2.0	180.1	46,883
	6	4	2.0	185.5	47,781
	7	4	2.0	189.8	45,509
	8	4	2.0	188.5	46,294
	9	4	2.0	182.3	45,348
	Mean			180.7	47,016
F20-H	1	3	2.0	192.0	49,465
	2	3	2.0	192.0	43,883
	3	4	2.0	177.5	40,806
	4	4	2.0	183.5	45,009
	5	4	2.0	166.5	43,537
	6	3	2.0	185.7	44,267
	Mean			181.9	44,267

Therefore, the mean compressive strength of the HSFRC with the hybrid steel fibers with lengths of 16.5 and 19.5 mm was not overall significantly different from that of the HSFRC with a single type of steel fiber with a length of 13 mm.

The results of the compressive strength tests on specimens with various steel fiber contents indicated that the incorporation of steel fiber content based on the concrete volume of less than 1.5% had a significant influence on the compressive strength of the HSFRC.

For the mixture with a single type of steel fiber, the F10-S-L130, F15-S-L130, and F20-S-L130 mixtures contained 1.0, 1.5, and 2.0% steel fibers based on the volume of concrete with a length of 13 mm, respectively. The compressive strength of each mixture was 173.0, 188.5, and 180.7 MPa, respectively. The compressive strength of the F15-S-L130 and F20-S-L130 specimens was 9.0 and 4.5% greater, respectively, than that of the F10-SL130 specimen. The elastic modulus value of the F10-S-L130, F15-S-L130, and F20-S-L130 specimens was 44,145, 45,996, and 47,016 MPa, respectively. The elastic modulus of the F15-S-L130 and F20-S-L130 specimens was 4.2 and 6.5% greater, respectively, than that of the F10-SL130 specimen.

For the mixture with hybrid steel fibers, the F10-H, F15-H, and F20-H mixtures contained 1.0, 1.5, and 2.0% hybrid steel fibers based on the concrete volume, respectively. The compressive strength of each mixture was 174.0, 181.2, and 181.9 MPa, respectively. The compressive strength of the F15-H and F20-H specimens increased by 4.1% and 4.5%, respectively, compared with the F10-H mixture. However, the compressive strength of the F20-H mixture was similar to that of the F15-H mixture. The elastic modulus of the F20-H specimen was 1.6% greater than that of the F10-H specimen.

4. Prediction of the Elastic Modulus

The elastic modulus was estimated by using a predictive equation from a design code and other equations that were suggested by researchers. The American Concrete Institute (ACI) 318-11 equation [15] for predicting the elastic modulus is based on the experimental results of normal-strength concrete. The ACI 363 committee [16] also proposed an equation for predicting the elastic modulus of concrete with a compressive strength of less than 83 MPa. Graybeal [12] proposed a prediction equation for the elastic modulus of HSFRC with a compressive strength of less than 200 MPa. Kakizaki [17] also proposed a prediction equation of the elastic modulus using the compressive strength of high-strength concrete. In this study, an elastic modulus prediction equation is proposed as follows:

$$E_c = 3,360 \times \sqrt{f'_c}, \quad (1)$$

where f'_c is the compressive strength of concrete (MPa).

The experimental results were compared with the predicted results of the elastic modulus by using the equations proposed in an earlier work and in this study. The elastic modulus predictions ($E_{c,cal}$) and experimental results ($E_{c,test}$) are shown in Figure 3. Table 5 shows the statistical data of the elastic modulus predicted values ($E_{c,cal}/E_{c,test}$) over the elastic modulus test results.

The mean $E_{c,cal}/E_{c,test}$ ratios using the proposed equations from ACI 318 and ACI 363 are 1.38 and 1.13, respectively, which overestimate the measured elastic modulus of the HSFRC because these proposed formulas are based on the elastic modulus test results using specimens with compressive strength of 100 MPa or less. The mean $E_{c,cal}/E_{c,test}$ ratios using Kakizaki's equation, Graybeal's equation, and the proposed equation in this study are 1.07, 1.13, and 0.99, respectively. Therefore, the equation proposed in this study more accurately predicts the elastic modulus of the HSFRC compared with the existing formulas.

5. Tensile Strength

5.1. Crack Mouth Opening Displacement Measurements. The tensile strength of concrete can be determined by either a direct tensile test or a crack mouth opening displacement

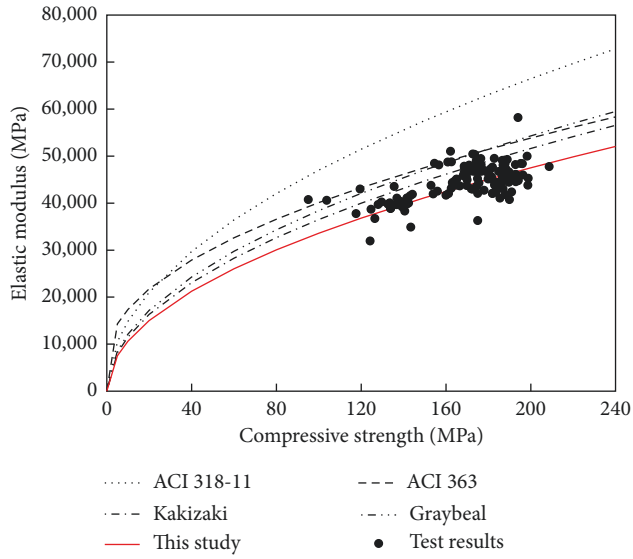

Figure 3: Prediction of the elastic modulus at various compressive strengths.

Table 5: Comparison of the test results and prediction of the elastic modulus.

Source	Equation	Range of compressive strengths	$E_{c,cal}/E_{c,test}$ Mean (m)	S.D. (σ)	C.O.V (σ/m)
ACI 318-11	$E_c = 4,700\sqrt{f'_c}$	—	1.38	1.16	0.84
ACI 363	$E_c = 3,320\sqrt{f'_c} + 6,900$	$f'_c \le 83$ MPa	1.13	0.82	0.73
Graybeal	$E_c = 3,840\sqrt{f'_c}$	$f'_c \le 200$ MPa	1.13	0.95	0.84
Kakizaki	$E_c = 3,650\sqrt{f'_c}$	$83 \le f'_c \le 138$ MPa	1.07	0.90	0.84
This study	$E_c = 3,360\sqrt{f'_c}$	$f_{ck} \le 200$ MPa	0.99	0.83	0.84

(CMOD) measurement method for a notched specimen. In the direct tensile test method, eccentricity at both ends of a specimen can cause variability in the experimental tensile strength results. Fracture mechanics factors such as toughness, energy release rate, and tensile strength of a steel fiber-reinforced concrete can be obtained by using CMOD measurement results of notched specimens.

RILEM [18] proposed a three-point load test method for measuring CMOD. In this study, a $100 \times 100 \times 400$ mm prismatic notched specimen was fabricated, and a three-point load bearing test was performed. The support distance of the specimen was 300 mm, and the load was applied at the center of the span. The notch machined into the center of the prismatic specimen had a depth of 10 mm and a width of 3.4 mm. A clip gauge with a capacity of 10 mm was attached to the end of the notch on the bottom, and the CMOD was measured at each load step (Figure 4). The load was applied by the displacement control method, and the displacement control speed was 0.2 mm/min. The tensile behavior of the HSFRC was analysed by using the CMOD measurement results.

5.2. CMOD Test Results. The comparison of the load-CMOD measurement of the F10-S-L130 and F10-H mixtures is shown in Figure 5, that of the load-CMOD measurement of the F15-S-L130 and F15-H mixtures in Figure 6, and that of the load-CMOD measurement of the F20-S-L130 and F20-H mixtures in Figure 7. The load-CMOD relationship curve increased linearly during the initial load step. After the initial cracking, the load nonlinearly increased and then the maximum load was reached. The CMOD at the maximum load was between 0.5 and 1.0 mm. The cracking resistance of the HSFRC was

Figure 4: Load-CMOD test setup.

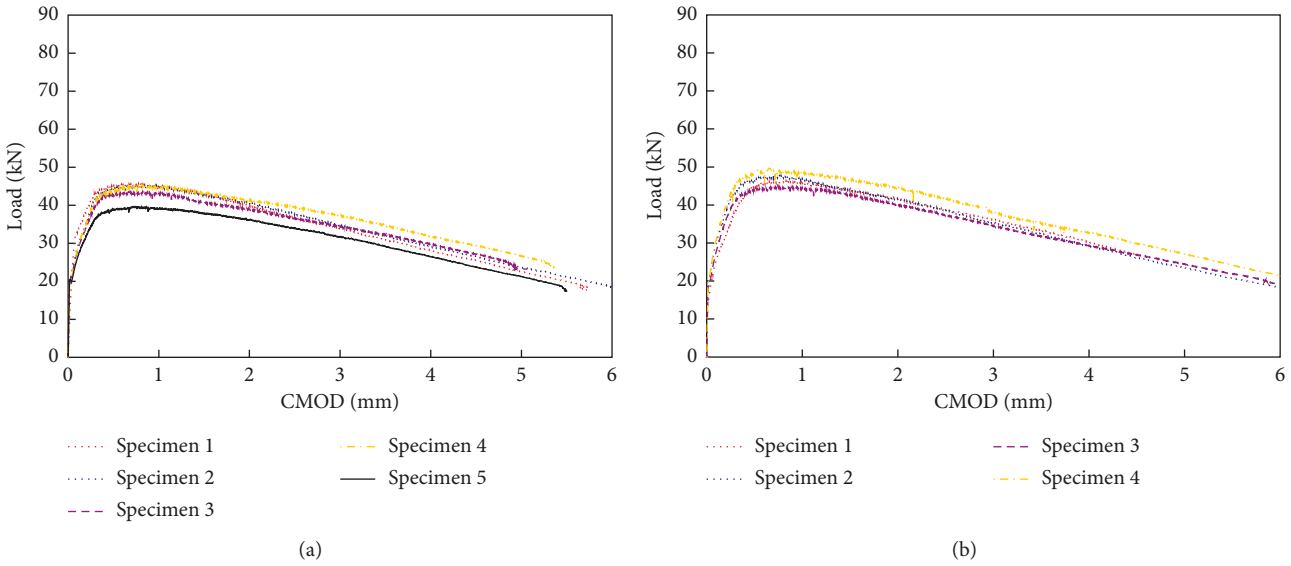

Figure 5: Comparison of the load-CMOD curves of the F10 series mixtures. (a) F20-S-L130 mixture. (b) F20-H mixture.

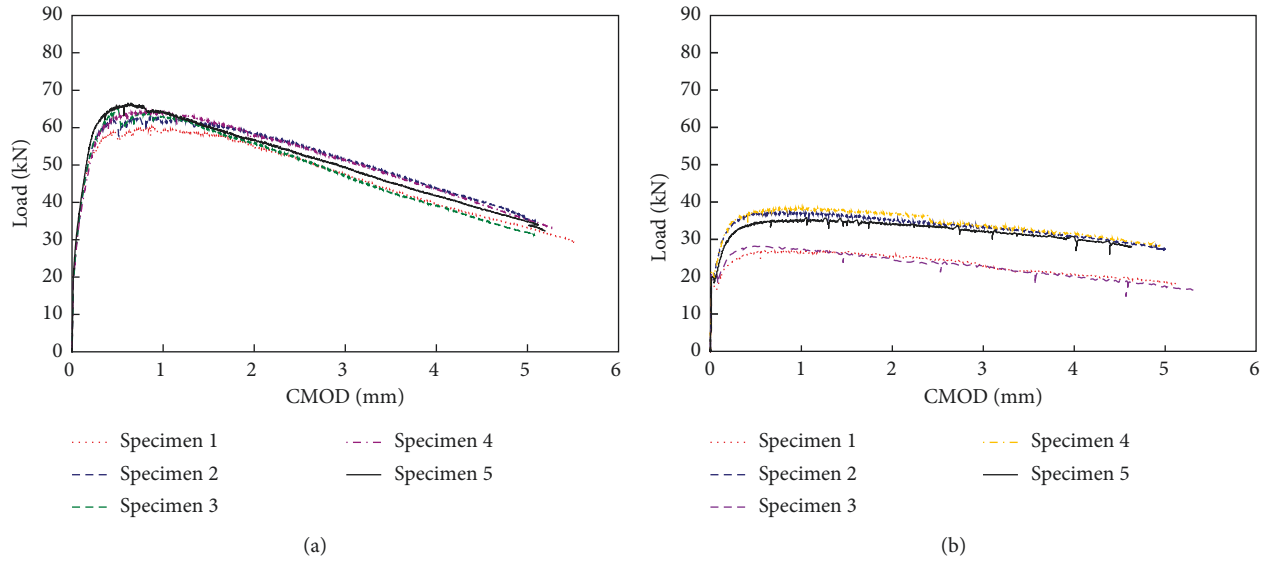

Figure 6: Comparison of the load-CMOD curves of the F15 series mixtures. (a) F10-S-L130 mixture. (b) F10-H mixture.

improved when the cracks occurred at the notch. Even after the maximum load was reached, the HSFRC exhibited a gradual tension-softening phenomenon without a sudden decrease in load because the HSFRC had a sufficient resistance to cracking due to the bridging effect of the steel fibers.

The variation of the maximum loads in each load-CMOD curve for the F10-S-L130, F15-S-L130, and F20-S-L130 mixtures with a single type of steel fiber was small. The variation of the maximum loads in each load-CMOD curve for the F10-H mixture with 1.0% hybrid steel fibers based on volume was also small. However, the variation of the maximum loads in each load-CMOD curve for the F15-H and F20-H mixtures with 1.5 and 2.0% hybrid steel fibers based on volume was greater than that of the maximum loads in each load-CMOD curve for the F10-H mixture. This result indicates that the combination of two types of steel fibers with more than 1.5% steel fiber content by volume might cause variations in the maximum loads during the CMOD test, which would accordingly influence the tensile strength of the UHFRC.

After the maximum load was reached, the load tended to decrease. The curves of the F15-S-L130 specimens decreased more sharply than those of the F15-H specimens, indicating that the longer hybrid fibers in the F15-H specimens became more active in crack bridging after the maximum load was reached. The short fibers in the F15-S-L130 specimens were pulled out earlier as the crack width increased.

The mean value of the maximum load in the CMOD test for the F10-S-L130, F10-S-L195, and F10-H mixtures was 45.1, 34.0, and 47.8 kN, respectively, as shown in Table 6.

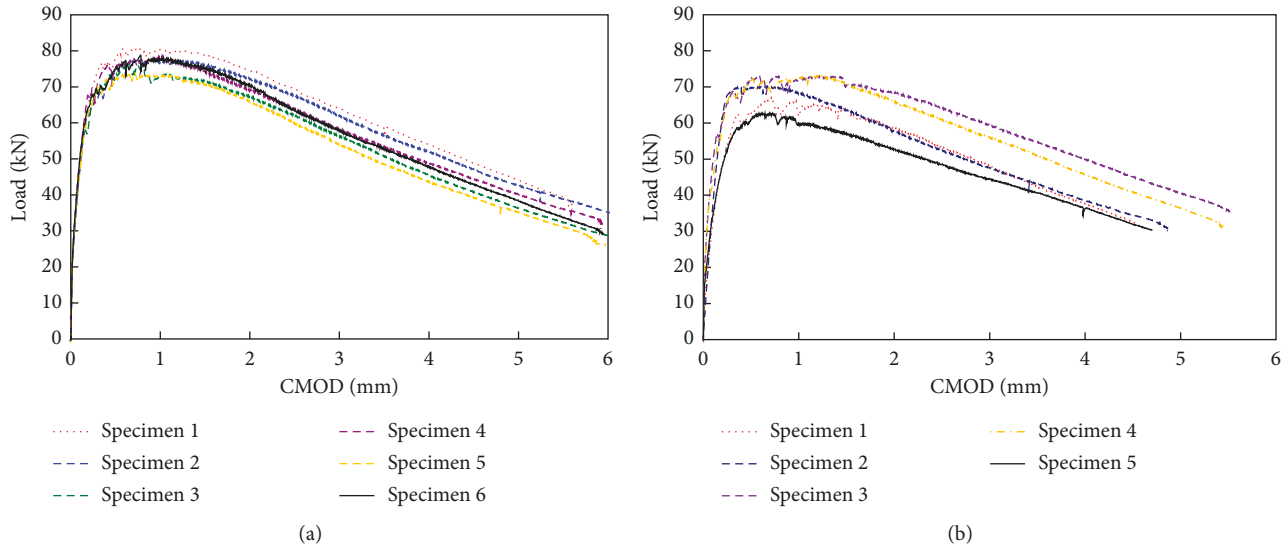

Figure 7: Comparison of the load-CMOD curves of the F20 series mixtures. (a) F15-S-L130 mixture. (b) F15-H mixture.

Table 6: Comparison of the test results and estimation from the regression analysis of the tensile strength (V_f = 1.0%).

Mixture	Batch	Number of specimens	Number of specimens successfully evaluated in the inverse analysis	Maximum load ($P_{max,mean}$) (kN)	Test result of the tensile strength ($f_{t,test}$) (MPa)	Prediction of the tensile strength ($f_{t,regression}$) (MPa)
F10-S-L130	1	5	4	48.8	10.07	10.31
	2	3	1	47.3	10.13	10.00
	3	5	2	43.8	8.86	9.25
	4	6	2	42.0	9.21	8.87
	Mean			45.1	9.61	9.53
F10-S-L195	1	4	3	46.6	9.65	9.84
	2	4	3	31.7	6.12	6.69
	3	4	2	30.2	6.22	6.39
	4	4	2	28.7	6.31	6.05
	5	3	2	32.6	7.07	6.88
	Mean			34.0	7.21	7.18
F10-H	1	5	2	47.8	9.85	10.09
	Mean			47.8	9.85	10.09

Since the blast-furnace slag was used as a binder in the F10-S-L195 mixture, the maximum load of the F10-S-L195 mixture was less than that of the other mixtures. The mean value of the maximum load in the CMOD test for the F15-S-L130, F15-H(BFS), and F15-H mixtures was 64.8, 35.5, and 37.4 kN, respectively, as shown in Table 7. The mean values of the maximum loads of the F15-H(BFS) and F15-H specimens were lower than that of the F15-S-L130 specimens, possibly due to an unfavourable orientation and dispersion of steel fibers in the F15-H(BFS) and F15-H mixtures. In addition, the mean value of the maximum load in the CMOD test for the F20-S-L130 and F20-H mixtures was 67.2 and 69.4 kN, respectively, as shown in Table 8. The CMOD measurement for each mixture group of F20 series was similar.

5.3. Tensile Strength. In this study, an inverse analysis was performed using the load-CMOD curve obtained in the experiment to determine the tensile stress-CMOD relationship. A virtual crack model from Hillerborg et al. [19] was used to perform the inverse analysis. The prismatic notched specimens were symmetrical with respect to the midspan of the specimen, so only half of the specimen was modelled numerically. The finite element mesh for the inverse analysis consisted of 1,076 triangular elements. The horizontal displacement of the midsection of the specimen in the finite element mesh was constrained because of the symmetric boundary condition, and the vertical displacement of the support was constrained. The detailed inverse analysis procedure using the load-CMOD relationship followed Yang et al. [20].

The tensile strength of the HSFRC was evaluated from the tensile stress-CMOD relationship. The tensile strength of each mixture group is shown in Tables 6–8. An iterative numerical procedure is required to evaluate the tensile stress by inverse analysis. The tensile stress could not be determined when the solution did not converge during the

Table 7: Comparison of the test results and estimation from the regression analysis of the tensile strength (V_f = 1.5%).

Mixture	Batch	Number of specimens	Number of specimens successfully evaluated in the inverse analysis	Maximum load ($P_{max,mean}$) (kN)	Test result of the tensile strength ($f_{t,test}$) (MPa)	Prediction of the tensile strength ($f_{t,regression}$) (MPa)
F15-S-L130	1	5	3	63.6	14.24	13.43
	2	5	4	64.8	13.86	13.69
	3	6	4	64.3	14.22	13.59
	4	5	3	66.6	14.49	14.07
	Mean			64.8	14.18	13.69
F15-H (BFS)	1	4	2	36.3	8.65	7.66
	2	4	2	34.7	9.48	7.32
	Mean			35.5	9.07	7.49
F15-H	1	6	3	55.7	11.65	11.76
	2	2	1	44.5	6.42	9.39
	3	6	2	40.9	7.35	8.65
	4	6	2	26.7	5.44	5.63
	5	5	1	25.1	5.94	5.29
	6	5	2	33.5	6.22	7.06
	Mean			37.4	7.76	7.89

Table 8: Comparison of the test results and estimation from the regression analysis of the tensile strength (V_f = 2.0%).

Mixture	Batch	Number of specimens	Number of specimens successfully evaluated in the inverse analysis	Maximum load ($P_{max,mean}$) (kN)	Test result of the tensile strength ($f_{t,test}$) (MPa)	Prediction of the tensile strength ($f_{t,regression}$) (MPa)
F20-S-L130	1	3	—	69.7	—	14.71
	2	4	3	60.0	12.73	12.67
	3	4	1	62.5	12.90	13.2
	4	4	3	63.3	13.10	13.36
	5	4	1	61.3	8.90	12.94
	6	4	2	72.0	15.00	15.21
	7	6	3	74.7	17.29	15.77
	8	6	4	79.7	17.15	16.83
	9	5	2	73.4	16.86	15.5
	Mean			67.2	14.92	14.18
F20-H	1	6	2	89.0	18.80	18.8
	2	3	1	70.1	14.69	14.8
	3	5	4	71.9	15.36	15.18
	4	6	2	62.6	13.38	13.21
	5	6	1	61.5	13.79	12.98
	6	6	4	62.3	13.58	13.16
	Mean			69.4	14.90	14.66

iterative calculation. The tensile stresses of the notched specimens that could not be obtained from the inverse analysis are omitted from Tables 6–8.

The number of specimens that were successfully evaluated in the inverse analysis of the F10-S-L130, F10-S-L195, and F10-H mixtures was 9, 12, and 2, respectively, and the mean tensile strength was 9.61, 7.21, and 9.85 MPa, respectively. The tensile strength of the F10-S-L195 mixture containing steel fibers with a length of 19.5 mm was less than that of the F10-S-L130 mixture containing steel fibers with a length of 13.0 mm. The tensile strength of the F10-H specimens was almost the same as that of the F10-S-L130 specimens but 36.6% greater than that of the F10-S-L195 specimens. The experimental results showed that the use of 16.5 and 19.5 mm hybrid steel fibers affected the tensile strength of the HSFRC as much as the use of a single type of steel fiber with a length of only 13 mm. However, the orientation and dispersion of using the 19.5 mm single-type steel fibers in the HSFRC were less advantageous than those of using the 13.0 mm single-type steel fiber, resulting in a decrease in the tensile strength of the HSFRC.

The numbers of specimens that were successfully evaluated in the inverse analysis of the F15-S-L130, F15-H (BFS), and F15-H mixtures with a steel fiber content of 1.5% were 14, 4, and 11, respectively, and these mixtures had mean tensile strength of 14.18, 9.07, and 7.76 MPa, respectively. The tensile strength of the F15-H specimens was reduced by 45.3% compared to that of the F15-S-L130 specimens.

In addition, the numbers of specimens that were successfully evaluated in the inverse analysis of the F20-S-L130 and F20-H mixtures with a 2.0% steel fiber content were 19 and 14, respectively, and these mixtures had mean tensile strength of 14.92 and 14.90 MPa, respectively. The

experimental results showed that the tensile strength of the HSFRC with 16.5 and 19.5 mm hybrid steel fibers was similar to that of the HSFRC using only 13.0 mm steel fibers. As discussed in the comparison of the F10-S-L130 and F10-H mixtures, the experimental results showed that in the case of the HSFRC containing a 2% steel fiber content based on the volume of concrete, the use of hybrid steel fibers with lengths of 16.5 and 19.5 mm affected the tensile strength of the HSFRC as much as the use of a single type of steel fiber with a length of only 13 mm.

Overall, the tensile strength obtained from the maximum load of the CMOD test and the inverse analysis of the CMOD test results of the F10-S-L195 and F15-H(BFS) mixtures was low because the blast-furnace slag binder decreased the tensile strength of the concrete, as mentioned previously.

The tensile strength of HSFRC was affected by the steel fiber content. The tensile strength of the F10-S-L130, F15-S-L130, and F20-S-L130 mixtures was 9.61, 14.18, and 14.92 MPa, respectively. The tensile strength of the F15-S-L130 and F20-S-L130 specimens was 47.6% and 55.3% greater, respectively, than that of the F10-SL130 specimen. The tensile strength of the specimens using the hybrid steel fibers was also affected by the steel fiber content. The tensile strength of the F20-H specimen was 51.3% higher than that of the F10-H specimen.

Since the tensile strength could not be obtained when the iterative calculation did not converge to a solution during the inverse analysis, determination of the tensile strength of each specimen with the inverse analysis using the load-CMOD relationship curve was limited. A regression analysis was performed with the maximum load from the load-CMOD test results, and the tensile strength obtained through the inverse analysis. The regression analysis was used to predict the tensile strength of the HSFRC. The predicted tensile strength from the regression analysis is as follows:

$$f_t = 0.21 \times P_t, \tag{2}$$

where f_t is the tensile strength of HSFRC (MPa) and P_t is the maximum load in CMOD measurement experiment (kN).

The relationship between the maximum load in the load-CMOD curve and the tensile strength of the specimens that were successfully determined in the inverse analysis using the CMOD experiment measurements is shown in Figure 8. The maximum load in the CMOD test has a nearly linear relationship with the tensile strength.

The tensile strength predicted using (2) for the CMOD measurements of all the prismatic specimens is shown in Tables 6–8. The mean values of the tensile strength predicted by the regression analysis of the F10-S-L130, F10-S-L195, and F10-H mixtures were 9.53, 7.18, and 10.09 MPa, respectively. The predicted tensile strength of the F15-S-L130, F15-H(BFS), and F15-H specimens was 13.69, 7.49, and 7.89 MPa, respectively. In addition, the predicted tensile strength of the F20-S-L130 and F20-H mixtures was 14.18 and 14.66 MPa, respectively. As shown in Tables 6–8, the tensile strength obtained from the inverse analysis and that calculated using the analytical regression formula agreed reasonably well. Therefore, the predictive equation from the regression analysis can accurately predict the tensile strength of HSFRC.

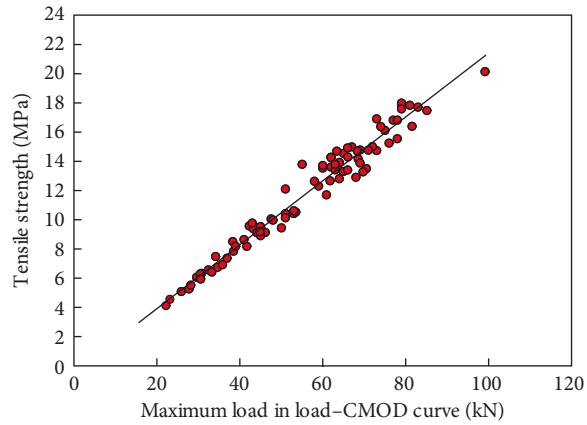

Figure 8: Comparison of the maximum loads in the load-CMOD curve with the tensile strength.

The tensile strength could not be directly obtained from the CMOD test results when the inverse analysis failed to obtain a solution. When tensile strength cannot be directly obtained through an inverse analysis, the tensile strength can be accurately predicted by using the formula proposed in this study without inverse analysis.

5.4. Relationship between Compressive Strength and Tensile Strength. Several equations have been proposed for predicting the tensile strength using the compressive strength of concrete [21–23]. However, most of these prediction equations are based on the experimental results of conventional concretes that do not include steel fibers or of normal-strength concrete with compressive strength less than 100 MPa. In addition, as shown in (3), most of the proposed equations are expressed as linear functions of the square root of the compressive strength with a coefficient related to the tensile strength:

$$f_{ct} = x\sqrt{f'_c}, \tag{3}$$

where x is the linear coefficient and f'_c is the compressive strength of concrete (MPa).

Graybeal [23] proposed a relationship between the compressive strength and tensile strength of ultrahigh-strength steel fiber-reinforced concrete based on the results of ultrahigh performance concrete with compressive strength greater than 150 MPa. In addition, curing methods were classified into three types, that is, steam curing, wet curing, and steam curing conditions with strengthening and retarding, and a unique linear coefficient value was defined for each curing method. Graybeal [23] suggested a coefficient of 0.65 for steam curing conditions, 0.56 for wet curing conditions, and 0.69 for steam curing conditions with strengthening and retarding.

The tensile strength of HSFRC is affected by the steel fiber content. Therefore, in this study, a prediction equation of the tensile strength is proposed by considering the compressive strength of the concrete as well as the steel fiber content as dependent variables. The proposed equation is as follows:

$$f_{ct} = 0.42(0.6 + V_f)\sqrt{f'_c}, \quad (4)$$

where V_f is the percent of steel fiber content based on the volume of concrete (%) and f'_c is the compressive strength of concrete (MPa).

The tensile strength predicted from Graybeal's equation and the tensile strength predicted from the proposed equation in this study are shown in Figure 9. For the prediction of the tensile strength using Graybeal's proposal formula, the linear coefficient of the steam curing conditions was 0.65. The predicted result from Graybeal's equation is approximately the predicted value of the tensile strength of HSFRC with a steel fiber content of 1.0%. Graybeal's equation also underestimates the tensile strength of HSFRC with steel fiber contents of 1.5 and 2.0%.

A comparison of the test results of tensile strength and the predicted tensile strength from the proposed equation in this study is shown in Figure 10. The tensile strength of steel fiber-reinforced concrete with various steel fiber contents could be more accurately predicted by using the equation proposed in this study.

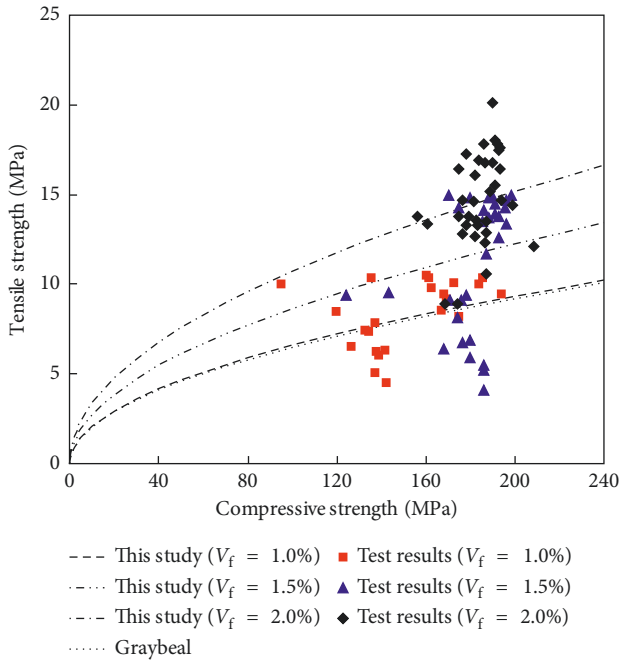

Figure 9: Prediction of the tensile strength by using the compressive strength and steel fiber content of the HSFRC.

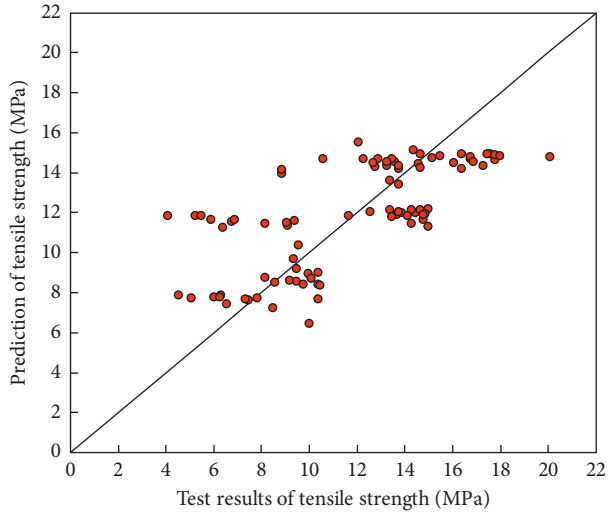

Figure 10: Comparison of the test results and prediction of the tensile strength.

6. Prediction of Material Properties Using the Steel Fiber Content

The effect of steel fiber content on the compressive strength, elastic modulus, and tensile strength of HSFRC was investigated, and a correlation equation was proposed. Figure 11 shows the compressive strength, elastic modulus, and tensile strength of the HSFRC with various steel fiber contents. As shown in Figure 11, although the steel fiber content is constant, the differences in the compressive strength, elastic modulus, and tensile strength values are considerable.

The compressive strength of the F10-S-L130, F10-S-L195, and F10-H mixtures with a steel fiber content of 1.0% is between 121.6 and 181.2 MPa, the elastic moduli are between 39,081 and 45,561 MPa, and the tensile strength is between 6.12 and 10.13 MPa. The compressive strength of the F15-S-L130, F15-H(BFS), and F15-H mixtures containing 1.5% steel fiber is between 132.5 and 188.5 MPa, the elastic moduli are between 39,123 and 48,334 MPa, and the tensile strength is between 5.44 and 14.49 MPa. The compressive strength of the F20-S-L130 and F20-H mixtures with a steel fiber content of 2.0% is between 158.2 and 192.5 MPa, the elastic moduli are between 40,806 and 49,465 MPa, and the tensile strength is between 12.67 and 18.80 MPa.

In addition, the maximum values of the compressive strength, elastic modulus, and tensile strength of the F20-S-L130 and F20-H mixtures with a steel fiber content of 2.0% are 192.0 MPa, 49,465 MPa, and 18.80 MPa, respectively. The minimum values of compressive strength, elastic modulus, and tensile strength are 158.2 MPa, 40,806 MPa, and 12.67 MPa, respectively.

The compressive strength, elastic modulus, and tensile strength of the F10-S-L195 and F15-H(BFS) mixtures that include blast-furnace slag as the binder are smaller than those of the other mixtures. Regression analysis was performed to evaluate the compressive strength, elastic modulus, and tensile strength prediction formulas according to the steel fiber content based on the volume of concrete as follows:

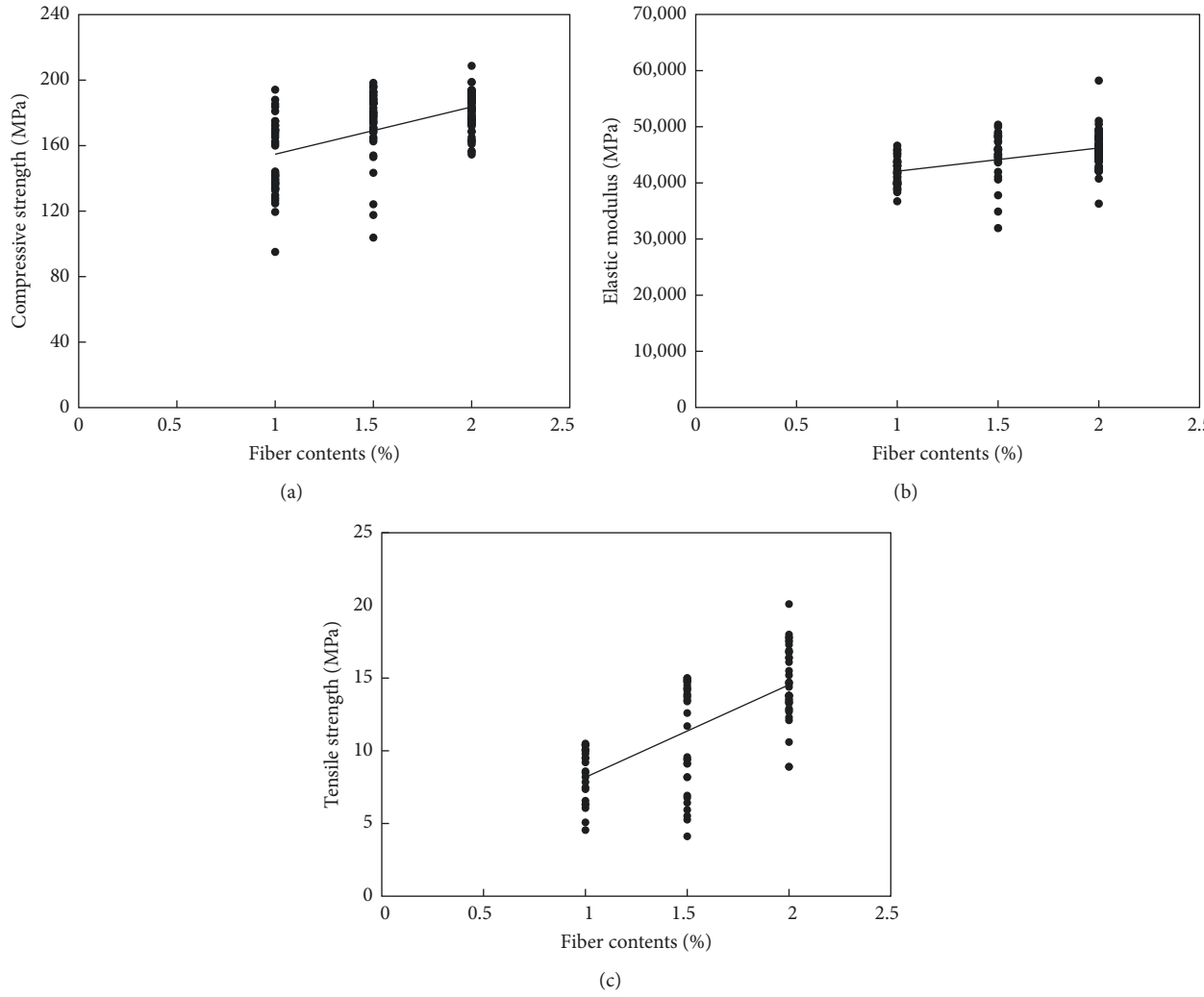

Figure 11: Mechanical properties according to the fiber contents. (a) Compressive strength. (b) Elastic modulus. (c) Tensile strength.

$$\begin{aligned} f'_c &= 28.86V_f + 125 \text{ (MPa)}, \\ E_c &= 4{,}150V_f + 37{,}900 \text{ (MPa)}, \\ f_t &= 6.36V_f + 1.82 \text{ (MPa)}, \end{aligned} \tag{5}$$

where f'_c is the compressive strength of the concrete (MPa), E_c is the elastic modulus (MPa); f_t is the tensile strength of the concrete (MPa), and V_f is the percent of steel fiber content based on the volume of concrete ($1.0 \le V_f \le 2.0$).

7. Conclusions

In this study, the compressive strength, elastic modulus, CMOD, and tensile strength of the HSFRC fabricated with a single type of steel fiber and the HSFRC fabricated with hybrid steel fibers were investigated. The main experimental results are as follows:

(1) In this study, steel fiber contents of 1.0, 1.5, and 2.0% were used to fabricate HSFRC. The compressive strength, tensile strength, and elastic modulus of the HSFRC increased with the steel fiber content. The compressive strength of the F15-S-L130 and F20-S-L130 specimens was 9.0 and 4.5% greater, respectively, than that of the F10-SL130 specimen. The elastic modulus of the F15-S-L130 and F20-S-L130 specimens was 4.2 and 6.5% greater, respectively, than that of the F10-SL130 specimen. The tensile strength of the F15-S-L130 and F20-S-L130 specimens was 47.6 and 55.3% greater, respectively, than that of the F10-SL130 specimen. The tensile strength of the HSFRC was most affected by the steel fiber content.

(2) The compressive strength, elastic modulus and tensile strength of the HSFRC containing steel fibers with a length of only 19 mm were measured and were found to be smaller than those of the mixtures containing steel fibers with a length of only 13.5 mm. The compressive strength of the F10-S-L130 and F10-S-L195 mixtures was 173.0 and 133.7 MPa, respectively, and the elastic modulus of the two mixtures was 44145 and 40147 MPa, respectively. In addition, the tensile strength of the two mixtures was

9.61 and 7.21 MPa, respectively. The different water-binder ratios of the two mixtures might be an important influential factor in the reduction of the compressive strength, elastic modulus, and tensile strength. In addition, the dispersion of steel fibers might affect these HSFRC mechanical properties. The decrease in compressive strength, elastic modulus, and tensile strength could result from the decrease in the dispersion of the steel fibers in the HSFRC due to the use of longer steel fibers.

(3) The experimental results of the compressive and tensile strengths of the HSFRC with hybrid steel fibers with lengths of 16.5 and 19.5 mm were similar to those of the HSFRC containing a single type of steel fiber with a length of only 13 mm. The mean compressive strength of the F10-S-L130, F15-S-L130, and F20-S-L130 mixtures containing a single type of steel fiber with a length of only 13 mm was 173.0, 188.5, and 180.7 MPa, respectively, and that of the F10-H, F15-H, and F20-H mixtures containing hybrid steel fibers was 174.0, 181.2, and 181.9 MPa, respectively. In addition, the mean tensile strength of the F10-S-L130 and F20-S-L130 mixtures was 9.61 and 14.92 MPa, respectively, and that of the F10-H and F20-H mixtures was 9.85 and 14.90 MPa, respectively. Therefore, in this study, the use of hybrid steel fibers was advantageous for ensuring the strength of HSFRC.

(4) A prediction equation that considers the compressive strength of HSFRC was proposed to predict the HSFRC elastic modulus. The equation suggested in this study accurately predicted the experimental results of the elastic modulus.

(5) An equation to predict the tensile strength of HSFRC was suggested using the maximum load obtained from the load-CMOD relationship. The prediction of tensile strength by using the proposed equation and the test results were approximately equal.

Additional Points

(i) An extensive experimental investigation of the mechanical properties of high-strength fiber-reinforced concrete (HSFRC) was carried out in this study.

(ii) The test parameters included a single type of steel fiber and hybrid steel fibers with lengths of 13, 16.5, and 19.5 mm and steel fiber contents of 1.0, 1.5, and 2.0% based on the volume of HSFRC.

(iii) The mechanical properties of the HSFRC with hybrid steel fibers were similar to those of the HSFRC with a single length of steel fiber.

(iv) Equations for predicting the elastic modulus and tensile strength of HSFRC were proposed based on the test results, and the predictions closely agreed with the experimental results.

Conflicts of Interest

The authors declare that they have no conflicts of interest.

Acknowledgments

This research was supported by a grant (13SCIPA02) from the Smart Civil Infrastructure Research Program funded by the Ministry of Land, Infrastructure and Transport (MOLIT) of the Korean government and the Korea Agency for Infrastructure Technology Advancement (KAIA).

References

[1] P. Rossi, A. Arca, E. Parant, and P. Fakhri, "Bending and compressive behaviors of a new cement composite," *Cement and Concrete Research*, vol. 35, no. 1, pp. 27–33, 2005.

[2] C. Magureanu, I. Sosa, C. Negrutiu, and B. Heghes, "Mechanical properties and durability of ultra-high-performance concrete," *ACI Materials Journal*, vol. 109, no. 2, pp. 177–184, 2012.

[3] K. Habel, M. Viviani, E. Denarié, and E. Brühwiler, "Development of the mechanical properties of an ultra-high performance fiber reinforced concrete (UHPFRC)," *Cement and Concrete Research*, vol. 36, no. 7, pp. 1362–1370, 2006.

[4] K. Wille, A. E. Naaman, S. El-Tawil, and G. J. Parra-Montesinos, "Ultra-high performance concrete and fiber reinforced concrete: achieving strength and ductility without heat curing," *Material and Structures*, vol. 45, no. 3, pp. 309–324, 2012.

[5] A. M. T. Hassan, S. W. Jones, and G. H. Mahmud, "Experimental test methods to determine the uniaxial tensile and compressive behavior of ultra high performance fiber reinforced concrete (UHFRC)," *Construction and Building Materials*, vol. 37, pp. 874–882, 2012.

[6] N. Banthia and R. Gupta, "Flexural response of hybrid fiber reinforced cementitious composites," *ACI Material Journal*, vol. 102, no. 5, pp. 382–389, 2005.

[7] S. H. Park, D. J. Kim, G. S. Ryu, and K. T. Koh, "Tensile behavior of ultra high performance hybrid fiber reinforced concrete," *Cement & Concrete Composite*, vol. 34, no. 2, pp. 172–184, 2012.

[8] N. Matsunaga, T. Nozawa, and H. Maeda, "Development of ultra high strength fiber-reinforced concrete (ESCON)," in *Proceedings of the 2017 fib Symposium, High Tech Concrete: Where Technology and Engineering Meet*, pp. 482–490, Springer, Cham, August 2017.

[9] Y. W. Chan and S. H. Chu, "Effect of silica fume on steel fiber bond characteristics in reactive powder concrete," *Cement and Concrete Research*, vol. 34, no. 7, pp. 1167–1172, 2004.

[10] N. Banthia and M. A. Tasdemir, "Toughness enhancement in steel fiber reinforced concrete through fiber hybridization," *Cement and Concrete Research*, vol. 37, no. 9, pp. 1366–1372, 2007.

[11] B. Akcay and M. A. Tasdemir, "Mechanical behavior and fiber dispersion of hybrid steel fiber reinforced self-compacting concrete," *Construction and Building Materials*, vol. 28, no. 1, pp. 287–293, 2012.

[12] B. A. Graybeal, "Compressive behavior of ultra-high-performance fiber-reinforced concrete," *ACI Materials Journal*, vol. 104, no. 2, pp. 146–152, 2007.

[13] D. Y. Yoo, S. T. Kang, and Y. S. Yoon, "Effect of fiber length and placement method on flexural behavior, tension-softening curve, and fiber distribution characteristics of

UHPFRC," *Construction and Building materials*, vol. 64, no. 14, pp. 67–81, 2014.

[14] S. J. Barnett, M. N. Soutsos, S. G. Millard, and J. H. Bungey, "Strength development of mortars containing ground granulated blast-furnace slag: effect of curing temperature and determination of apparent activation energies," *Cement and Concrete Research*, vol. 36, no. 3, pp. 434–440, 2006.

[15] American Concrete Institute (ACI), *Building Code Requirements for Structural Concrete and Commentary*, Report ACI 318-11, American Concrete Institute, Farmington Hills, MI, USA, 2011.

[16] ACI Committee 363, *Report on High-Strength Concrete (ACI 363R-92)*, American Concrete Institute, Farmington Hills, MI, USA, 1992.

[17] M. Kakizaki, *Effect of Mixing Method on Mechanical Properties and Pore Structure of Ultra High-Strength Concrete*, Katri Report no. 90, Kajima Corporation, Tokyo, Japan, 1992.

[18] RILEM TC 162-TDF, "Test and design methods for steel fiber reinforced concrete; bending test-final recommendation," *Material and Structures*, vol. 35, no. 253, pp. 579–582, 2002.

[19] A. Hillerborg, M. Modeer, and P. E. Petersson, "Analysis of crack formation and crack growth in concrete by means of fracture mechanics and finite elements," *Cement and Concrete Research*, vol. 6, no. 6, pp. 773–782, 1976.

[20] I. H. Yang, C. B. Joh, and B. S. Kim, "Flexural response predictions for ultra-high-performance fiber-reinforced concrete beams," *Magazine of Concrete Research*, vol. 64, no. 2, pp. 113–127, 2011.

[21] J. Thomas and A. Ramaswamy, "Mechanical properties of steel fiber-reinforced concrete," *Journal of Materials in Civil Engineering*, vol. 19, no. 5, pp. 385–392, 2007.

[22] P. S. Song and S. Hwang, "Mechanical properties of high-strength steel fiber-reinforced concrete," *Construction and Building Materials*, vol. 18, no. 9, pp. 669–673, 2004.

[23] B. A. Graybeal, *Material Property Characterization of Ultra High Performance Concrete*, Report No. FHWA-HRT-06-103, FHWA, U.S. Department of Transportaion, McLean, VA, USA, 2006.